COSMOLOGICAL PARAMETERS & DARK MATTER: THE STATUS

Einstein Equation:

$$\Omega + \lambda - K = 1$$

$$q = \Omega/2 - \lambda$$

$$H = \dot{a}/a; \qquad \Omega = \rho/\rho_{\rm crit}; \qquad \lambda = \Lambda/3H^2$$

$$q = -\ddot{a}a/\dot{a}^2 \qquad K = k/a^2H^2$$

The value at the present epoch: H_0, Ω_0, λ_0 fix completely the evolution of the universe

Other parameters:

global: Ω_b; T_0(CMB)

perturbations: n_s; σ_8; T/S

Theorists' Paradigm as of 1990±7

$H_0 = 50\ \mathrm{km^{-1}s^{-1}Mpc^{-1}}$

$\Omega = 1$

$\Lambda = 0$

Theorists' Paradigm as from 1999

$H_0 = 70\ \mathrm{km^{-1}s^{-1}Mpc^{-1}}$

$\Omega = 0.3$

$\Lambda = 0.7$

Hubble Constant

Thesis: How to estimate

$$H_0 = (v - v_p)/d, \qquad v = cz$$

$m - M = 5\log(d/10\text{pc})$: distance modulus

The main task: to find good "standard" candles
(distance indicators)

main sequence stars; Cepheid P-L relation;

supernovae Ia (SNeIa); Tully-Fisher relation, ...

– All indicators are applicable to distance scales of restricted ranges

Invoke "*Distance Ladders*"

"Physical" methods (no ladders)

SNeII Expansion parallax (Baade-Wesselink method);

gravitational lensing; Sunyaev-Zeldovich effect;

Cosmic Microwave Background

— problem: how to know systematic errors

Distance Ladder

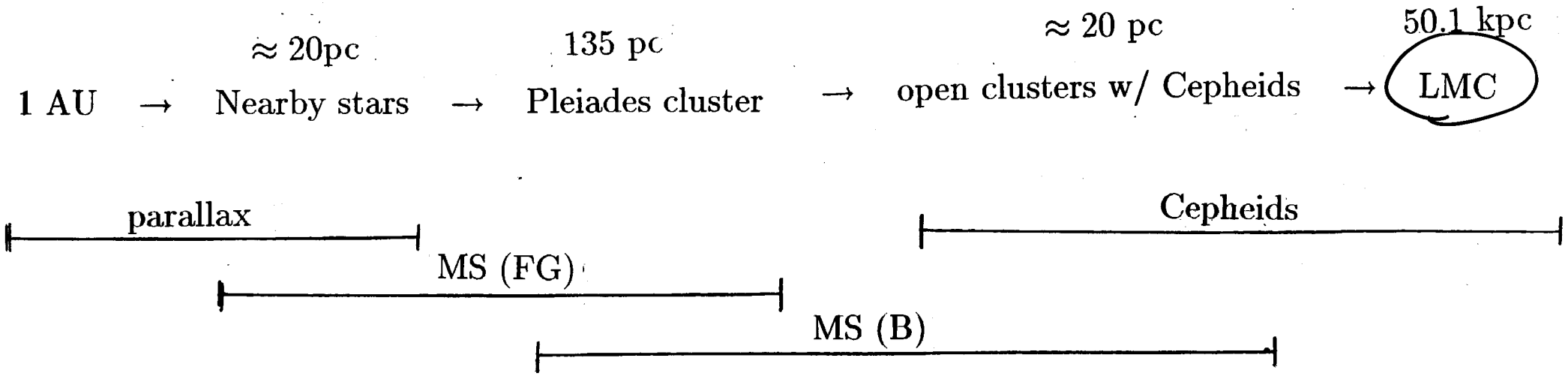

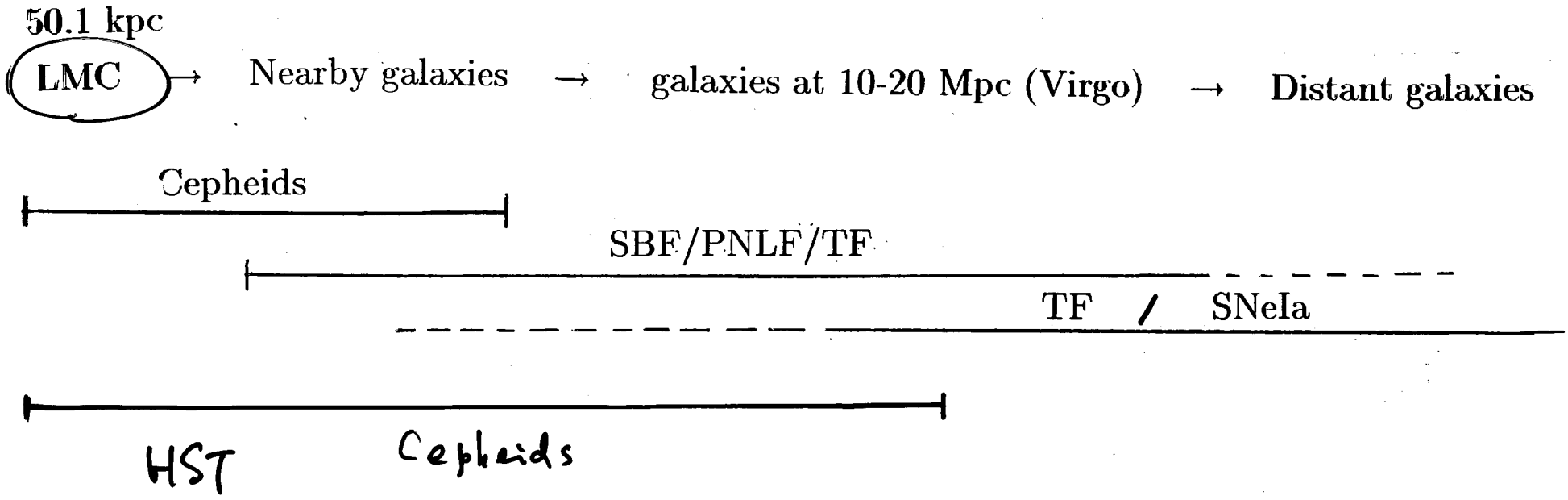

Historical Survey

I pre-WW II period

Leavitt (1912), Shapley, Hubble (1923+)

Baade (1952)

II pre-1985 Sandage × de Vaucouleurs

$H_0 = 50 - 100$

LMC distance "converged" to 50 kpc

III 1986-1990 $H_0 = 50 - 90$

Tully-Fisher relation (1977) :

$\log L = 2.5 \log v_{\rm circ}$+constant

(a) Take TF result as it is, or

(b) Large corrections to TF

IV 1990-1994 $H_0 = 50 \pm 5$ or 80 ± 10

more secondary indicators found:

PNLF, SBF, Type II SNe

& cross correlations among them $H_0 = 80 \pm 10$

Type Ia SNe: calib w/ model $H_0 = 50 \pm 5$

Type Ia SNe: calib w/ Cepheids (HST) $H_0 = 55 \pm 5$

Tonry et al 6

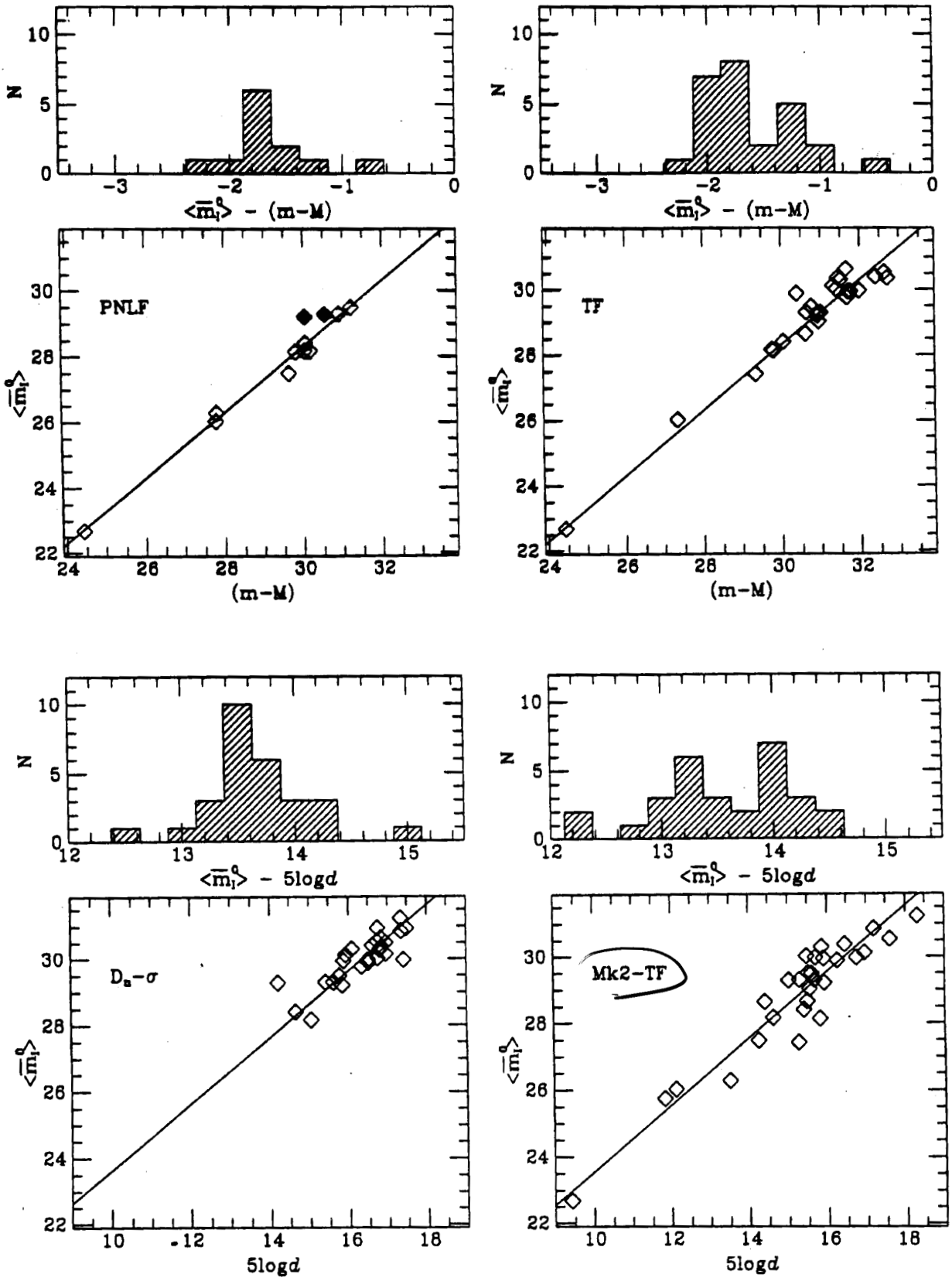

FIG. 7.—Same as Fig. 6, but comparing SBF and the tertiary estimators PNLF, TF (Mpc zero point), TF (from Mark II catalog), and D_n-σ. PNLF distances for the Coma I and II galaxies are plotted as solid symbols.

V 1994-Present $H_0 = 70 \pm 10$

Cepheids (HST): drastic increase of #Cepheid calibrators for secondary indicators $H_0 = 75 \pm 10$

SNeIa are *not* a standard candle, but depend on the decline rate $H_0 = 65 \pm 10$

1997 Hipparcos:
posed problems with local calibrations

2000 HST-KP

Reanalysis: Saha-Sandage observations of Cepheids + Corrections for heavy element abundance effects

$\rightarrow$ 10% upward shift of Cepheid distance of SNeIa host galaxies: $H_0 = 65 \rightarrow 71$

2002 value of the HST-KP team $H_0 = 72 \pm 8$

Problems remained

Galactic distance scale to LMC

Independent analysis needed

Cepheid Distance

ID	membership	$(m-M)_0$	T(RC3)	[O/H]*	
N224 (M31)	LG	24.42(12)	3	0.48(15)	ground
N300	Sculptor	26.70(11)	7	-0.15(15)	ground
N598 (M33)	LG	24.63(9)	6	0.32(15)	ground
N2403	M81	27.51	6	0.05	ground
N3109		25.50(20)	9	-0.44(15)	ground
N3031 (M81)	M81	27.80(18)	2	0.25(15)	HST-KP
N5457 (M101)	M101	29.35(17)	6	0.02	HST-KP
N925	N1023	29.84(16)	7	0.05(15)	HST-KP
N3351 (M95)	Leo I	30.01(19)	3	0.74(20)	HST-KP
N3621		29.17(18)	7	0.24	HST-KP
N4321 (M100)	Virgo	31.03(17)	4	0.63(20)	HST-KP
N1365	Fornax	31.43(20)	3	0.46(20)	HST-KP
N3368 (M96)	Leo I	30.27(13)	2	0.70(20)	British
N4496A	Virgo	31.13(10)	8	0.00	HST-SNeI
N4571	Virgo	30.87(15)	6.5		*CFHT*
N4536	Virgo	31.10(13)	4	0.00	HST-SNeI
N4639	Virgo-Wcl	32.00(23)	4	0.10	HST-SNeI
I4182		28.36(9)	9	−0.35	HST-SNeI
N5253		27.93(16)	10	−0.35(15)	HST-SNeI
N7331		30.89(16)	3	0.35	HST-KP
N4725	Coma I-II	30.50(16)(17)	2	0.47	HST-KP
N2541	N2841	30.47(11)(12)	6	−0.20	HST-KP
N4535	Virgo	31.02(26)	5		HST-KP
N2090	Virgo	30.45(16)(16)	5		HST-KP
N4548(M91)	Virgo	31.01(28)	2		HST-KP
N4603	Centaurus	32.61(11)(25)	5		Newman
N1326A	Fornax	31.36(0.17)(0.13)	9		HST-KP
N3319		30.78(14)(10)	6		HST-KP
N4414			5		HST-KP
N1425			3		HST-KP
N3198			5		HST-KP

[O/H]* is the value with respect to LMC [O/H]=−0.40

0.4 dex added to ⊙ value

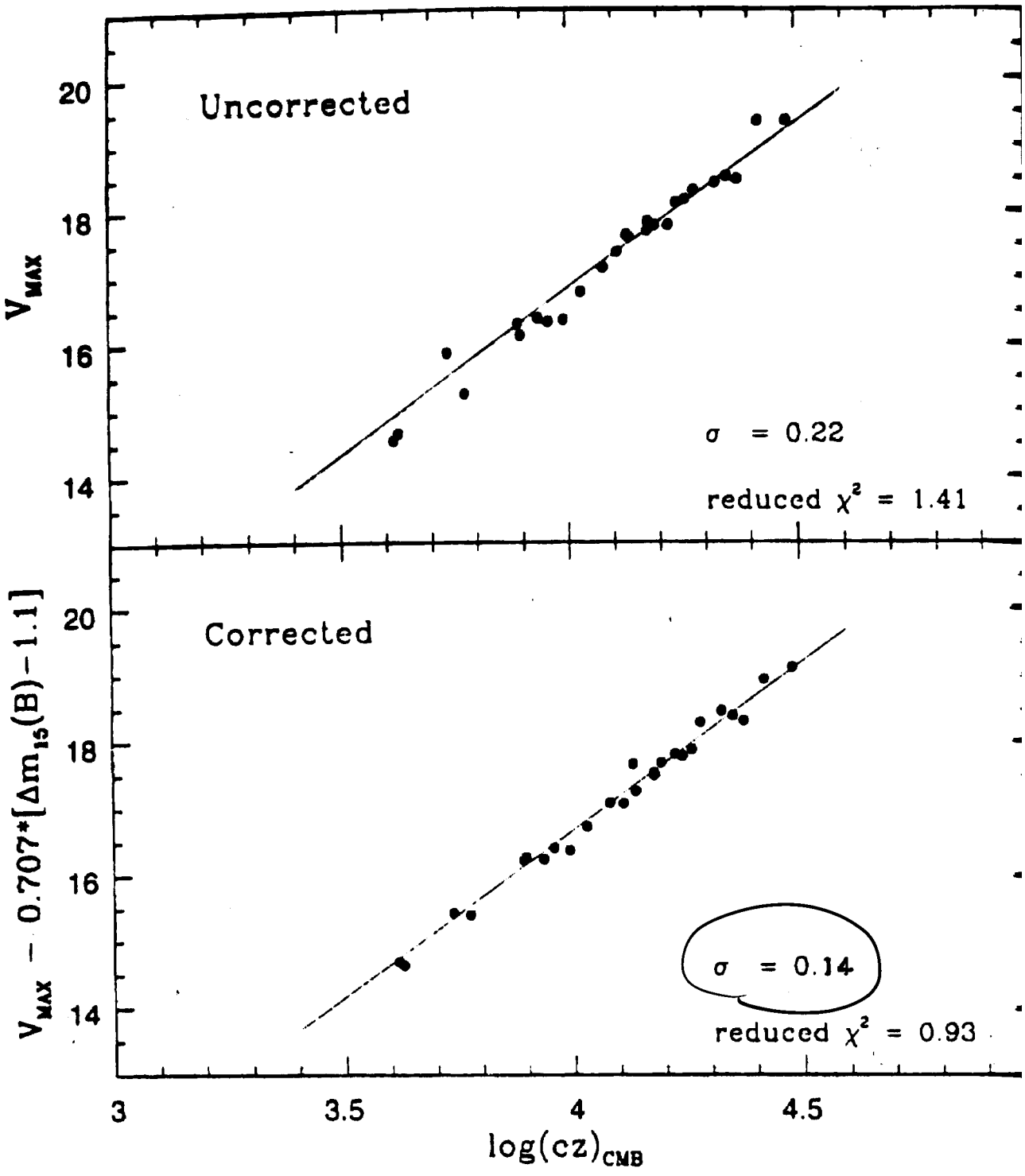
Uncorrected
σ = 0.22
reduced χ² = 1.41
Corrected
σ = 0.14
reduced χ² = 0.93
V_MAX
V_MAX − 0.707*[Δm15(B)−1.1]
log(cz)CMB
20
18
16
14
3
3.5
4
4.5

	HST-KP value	other analyses
Local Hubble diagram	(75±10)	85±5[a]
Type Ia SNe	71±2±6	74±2±4[b]
Tully-Fisher	71±3±7	83±8[c]
SBF	70±5±6	83±4±7[d]
Type II SNe	72±9±7	
FP relation	82±6±9	
	72±3±7	

NB: All works assume $(m - M)_{LMC} = 18.5 \pm 0.1$ (d=50.1 kpc)

(a) Willick & Batra: new photometry (+5% shift) and a different flow model

(b) Suntzeff et al. zero point w/ new HST-KP value

(c) Tully & Pierce zero point w/ new HST-KP value

(d) Blakeslee et al. zero point w/ new HST-KP value

Independent analyses, incl. Cepheid photometry, are needed

LMC distance

HST-KP takes it to be $(m - M) = 18.5 \pm 0.1$ (5% error)

But estimates vary from $\underset{(-15\%)}{18.2} - \underset{(+5\%)}{18.6}$

Pleiades problem after Hipparcos

geometric calibration of the HST Cepheid distance

NGC 4258: habours hydrogen maser

maser distance	7.2±0.5 Mpc
Cepheids (1999)	8.1±0.4 Mpc
Cepheids (2001)	7.8±0.3±0.5 Mpc

only one case so far.

More geometric/semi-geometric methods

Wait for GAIA for the definitive solution

LMC distance before 1997

Cepheid		
optical	PL	18.50 +/- 0.07
IR	PL	18.55 +/- 0.07
Mira		18.48
SN 1987A Ring echo		18.50 +/- 0.13
SN 1987A EPM		18.45 +/- 0.21
RR Lyrae		18.23 ✓
Best value to LMC		18.50 +/- 0.15 → 7%

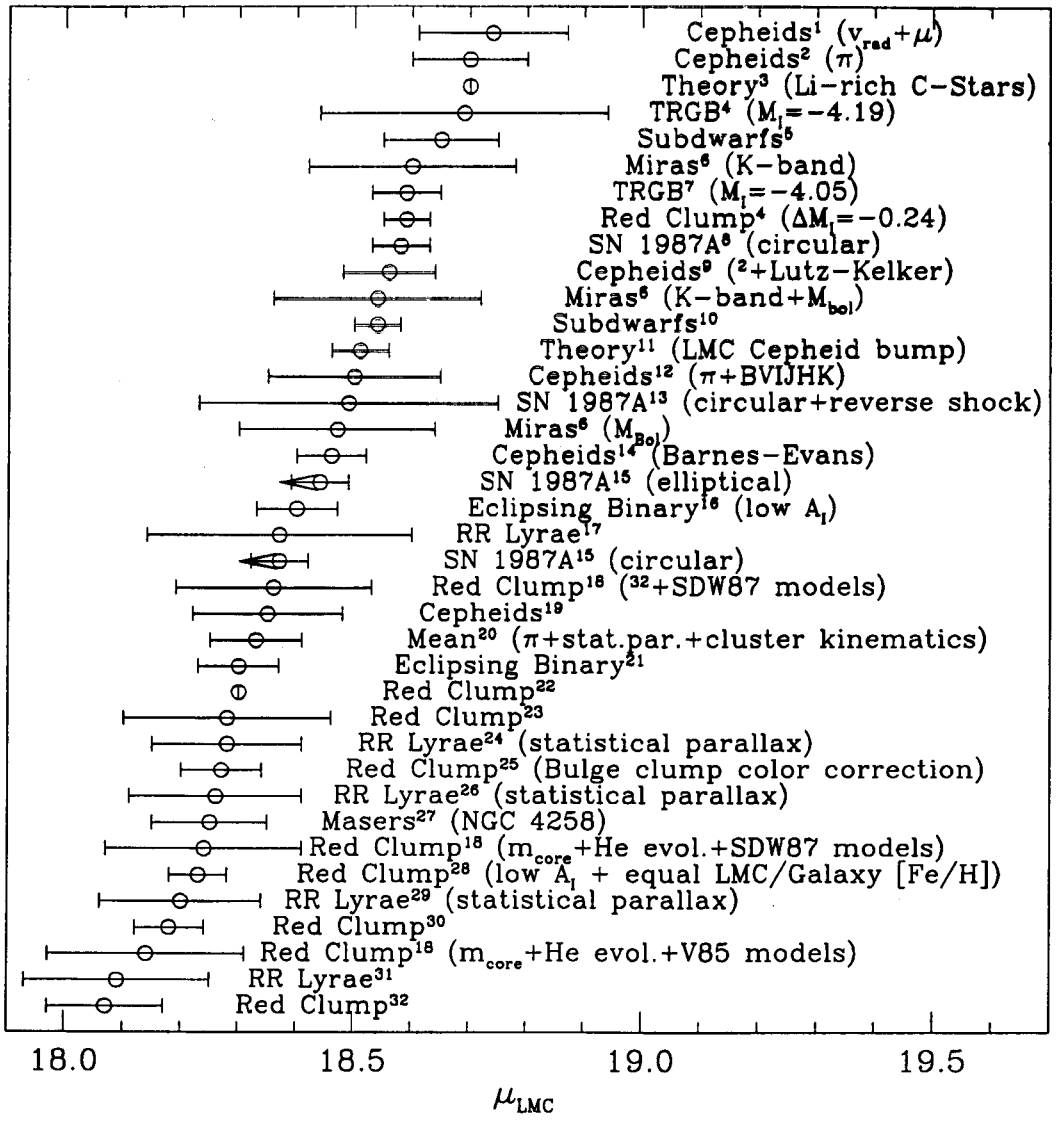

Fig. 1. Compilation of recent distance determinations to the LMC, presented in decreasing order of modulus μ_{LMC}. Cepheids, fitting to local Galactic subdwarf sequences, and theoretical stellar models tend to favor the "long" distance scale (i.e., $\mu_{LMC} \gtrsim 18.5$, while RR Lyrae, red clump luminosities, eclipsing binaries, and masers (indirectly, through NGC 4258) tend to favor the "short" scale (i.e., $\mu_{LMC} \lesssim 18.4$). References: [1]Feast et al. (1998); [2]Feast & Catchpole (1997); [3]Ventura et al. (1999); [4]Romaniello et al. (1999); [5]Reid (1997); [6]van Leeuwen et al. (1998); [7]Sakai et al. (2000); [8]Panagia (1998); [9]Oudmaijer et al. (1998); [10]Caretta et al. (1999); [11]Wood (1998); [12]Madore & Freedman (1998); [13]Garnavich et al. (1999); [14]Gieren et al. (1998); [15]Gould & Uza (1998); [16]Nelson et al. (1999); [17]Luri et al. (1998); [18]Cole (1998); [19]Luri et al. (1999); [20]Popowski & Gould (1999); [21]Guinan et al. (1998); [22]Beaulieu & Sackett (1998); [23]Girardi et al. (1998); [24]Layden et al. (1996); [25]Fernley et al. (1998); [26]Popowski (1999); [27]Maoz et al. (1999); [28]Udalski (1999); [29]Popowski & Gould (1998) and Gould & Popowski (1998); [30]Udalski (1998b); [31]Udalski (1998a); [32]Stanek et al. (1998).

14

a misalignment is not uncommon between galaxies and their cores. But the spin axis of the disk is parallel, at least in projection, to the Hα and radio synchrotron jets[22] emanating from the nucleus on the scale of 500 pc. The molecular disk and helical strands have the same sense of rotation. We point out that there are systematic deviations from the simple disk model presented here, such as the departure from a linear dependence of the systematic features below 460 km s^{-1} (Fig. 3 inset) and the deviations in the declinations of the high-velocity features from planar geometry (Fig. 2). The former effect is probably due to a slight fluctuation in the radii of the masers in that part of the disk (Fig. 2c). The latter effect is probably due to a warp[23,24] or other distortion. It can be modelled as a series of concentric rings with constant inclination but with a progression in the line of nodes of ~6°. None of the parameters in Table 1 are significantly affected.

Spectroscopic studies[6,7] over several years show that the systemic features drift at a rate of 9.5 ± 1.1 km s^{-1} yr^{-1}. Given the inner rotational velocity of 1,080 km s^{-1}, the velocity drift is undoubtedly due to the centripetal acceleration of gravity, $\dot{V} = V^2/R$ (where V is the rotational velocity at the inner radius R), from which we infer a linear radius of 0.13 pc. Combined with our angular size of 4.1 mas, we estimate the distance to be 6.4 ± 0.9 Mpc. Previous estimates have ranged from 3.3 to 7 Mpc (ref. 25). Our distance estimate is based on a direct geometric method, that is independent of the usual hierarchy of distance estimators. Its further refinement may help to improve the cosmic distance scale.

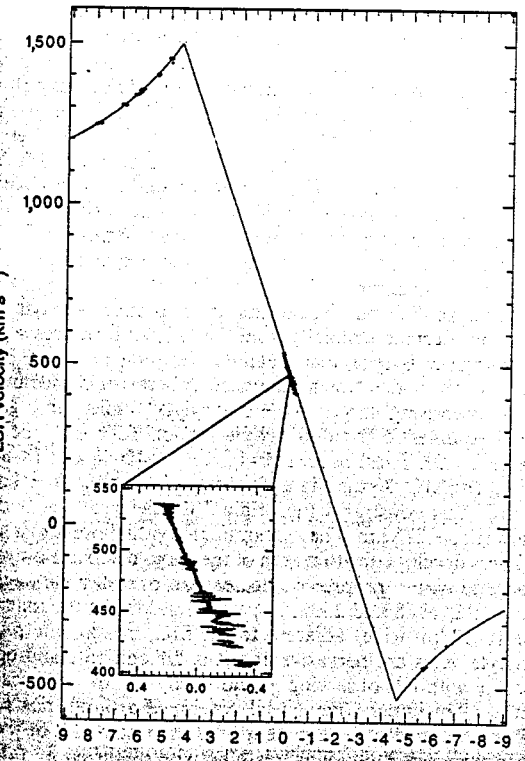

FIG. 3 Line-of-sight velocity versus distance along the major axis (position angle, 86°). Inset, data near the systemic velocity of the galaxy. The position errors are only visible on the scale of the inset. The line is derived from a model whose parameters are listed in Table 1. The high-velocity emission regions define keplerian orbits and constrain the estimate of the enclosed mass. The linear dependence of the systemic emission is a consequence of the change in projection of the rotation velocity.

TABLE 1 Parameters of molecular disk traced by water-vapour masers

Inner radius	4.1 mas (0.13 pc)*
Outer radius	8.0 mas (0.25 pc)*
Inner rotation velocity	1,080 ± 2 km s^{-1}
Outer rotation velocity	770 ± 2 km s^{-1}
Inner rotation period	750 yr
Outer rotation period	2,100 yr
Position angle	86 ± 2°
Inclination	83 ± 4°
Position velocity slope (dr/dv)	3.89 ± 0.01 microarcsec per (km s^{-1})
Central mass	3.6 × 10^7 $M_\odot$
Disk mass	<4 × 10^6 $M_\odot$
Central mass density	>4 × 10^9 $M_\odot$ pc^{-3}
Centripetal acceleration†	9.5 ± 1.1 km s^{-1} yr^{-1}
Disk systemic velocity‡	476 ± 2 km s^{-1}
Galactic systemic velocity‡§	472 ± 4 km s^{-1}
Radial motion	<10 km s^{-1}
Thickness of disk	<0.003 pc
Maser beam angle	7°
Disk–galaxy angle‖	119°
Apparent maser luminosity	110 $L_\odot$
Model luminosity¶	7 $L_\odot$
Distance	6.4 ± 0.9 Mpc

* Based on the distance estimate of 6.4 Mpc.
† From Greenhill *et al.*[8].
‡ Radio definition, and with respect to the local standard of rest. To convert to heliocentric velocity (radio), subtract 8.2 km s^{-1}; to convert to heliocentric (optical), subtract 7.5 km s^{-1}.
§ From Cecil *et al.*[16].
‖ Angle between the spin axis of the molecular disk and the spin axis of the galaxy[16,26].
¶ Radiation into a zone within 4° of the plane of the disk.

The high-velocity features have velocity drifts of <1 km s^{-1} (refs 6, 7) as expected if they lie on the mid-line of the disk. They should also have small proper motions. The systemic features, however, should show proper motions of 35 microarcsec yr^{-1}. These could be readily measured in future VLBI observations in order to improve the definition of the disk and to estimate the distance more accurately. □

Received 2 December; accepted 21 December 1994.

1. Rees, M. J. *A. Rev. Astr. Astrophys.* **22,** 471–506 (1989).
2. Begelman, M. C., Blandford, R. D. & Rees, M. J. *Rev. mod. Phys.* **56,** 255–351 (1984).
3. Claussen, M. J., Heiligman, G. M. & Lo, K. Y. *Nature* **310,** 298–300 (1984).
4. Claussen, M. J. & Lo, K. Y. *Astrophys. J.* **308,** 592–599 (1986).
5. Nakai, N., Inoue, M. & Miyoshi, M. *Nature* **361,** 45–47 (1993).
6. Greenhill, L. J. *et al. Astrophys. J.* (in the press).
7. Haschick, A. D., Baan, W. A. & Peng, E. W. *Astrophys. J.* **437,** L35–L38 (1994).
8. Greenhill, L. J., Henkel, C., Becker, R., Wilson, T. L. & Wouterloot, J. G. A. *Astr. Astrophys.* (in the press).
9. Watson, W. D. & Wallin, B. K. *Astrophys. J.* **432,** L35–L38 (1994).
10. Zensus, J. A., Diamond, P. J. & Napier, P. J. *VLBI Summer School* (Astr. Soc. Pacific, San Francisco, in the press).
11. Frank, J., King, A. & Raine, D. *Accretion Power in Astrophysics* 74 (Cambridge Univ. Press, 1992).
12. Ford, H. C. *et al. Astrophys. J.* **435,** L27–L30 (1994).
13. Harmes, R. J. *et al. Astrophys. J.* **436,** L35–L38 (1994).
14. Kormendy, J. & Richstone, D. *Astrophys. J.* **393,** 559–578 (1992).
15. Eckart, A., Genzel, R., Hofman, R., Sams, B. J. & Tacconi-Garman, L. E. *Astrophys. J.* **407,** L77–L80 (1993).
16. Cecil, G., Wilson, A. S. & Tully, R. B. *Astrophys. J.* **390,** 365–377 (1992).
17. Lonsdale, C. J., Diamond, P. J., Smith, H. E. & Lonsdale, C. J. *Nature* **370,** 117–120 (1994).
18. Haschick, A. D. *et al. Astrophys. J.* **356,** 149–155 (1990).
19. Turner, J. L. & Ho, P. T. P. *Astrophys. J.* **421,** 122–139 (1994).
20. Henkel, C. *et al. Astr. Astrophys.* **141,** L1–L3 (1984).
21. Neufeld, D. A., Maloney, P. R. & Conger, S. *Astrophys. J.* **436,** L127–L130 (1994).
22. Cecil, G., Wilson, A. S. & DePree, C. *Astrophys. J.* (in the press).
23. Binney, J. *A. Rev. Astr. Astrophys.* **30,** 51–74 (1992).
24. Arnaboldi, M. & Galletta, G. *Astr. Astrophys.* **268,** 411–417 (1993).
25. Courtès, G. *et al. Astr. Astrophys.* **268,** 419–442 (1993).
26. Hubble, E. *Astrophys. J.* **97,** 112–118 (1943).

ACKNOWLEDGEMENTS. We thank G. Cecil, K. Kellermann, J. Kormendy, T. Nakano, M. Reid, R. Schild and B. Schmidt for helpful discussions. M. Miyoshi thanks the Foundation for the Promotion of Astronomy of Japan and the Smithsonian Institution for travel support. The VLBA and VLA are facilities of the National Radio Astronomy Observatory, which is operated by Associated Universities, Inc., under a cooperative agreement with the US NSF.

Miyoshi et al.

Physical Methods

1. Expansion parallaxes of SNe II

   Model optical luminosity versus observed flux

2. Gravitational lensing: time delay

$$\Delta t \propto \frac{1}{H_0}(\Delta\theta_{ij}^2 - \Delta\Psi_{ij})$$

4 Lenses yield $H_0 = 74 \pm 8$ (Koopmans & Fassnacht)
B0218+357; Q0957+561; B1608+656; PKS1830-211

Systematic errors from mass models?

3. Sunyaev-Zeldovich effect

   cluster depth from SZ vs. cluster size from X ray

   Systematic errors:

   spherical assumption

   cluster model-profile dependence

For the future:

gravitational waves from binary coalescences (?)

Age of the Universe

1. Turn-off luminosity of Main Sequence stars in globular clusters

— Estimates vary from 11 Gyr to 18 Gyr

1) Uncertainty in the LMC distance with RR Lyrae

$$t \propto L^{-1} \propto d^{-2}$$

2) Interpretation of the age-metallicity corrections of the globular cluasters

formation is coeval, or non-coeval

To resolve uncertainties:

— More studies for the zero point of RR Lyrae stars

— Verification of the mass-luminosity relation (do-able)

2. Position of the first peak of C_ℓ of CMB

$\ell = 220$ contour nearly coincides with 13-14 Gyr isochronal contour

$$t_0 = 13.6 \pm 0.2 \text{ Gyr}$$

MATTER CONTENT OF THE UNIVERSE

Evidence for the Dark Matter revisited

Mass in clusters: $M/L = (250 - 450)h$ in units of solar

velocity dispersion

Zwicky 1933

CNOC Collaboration 1997

X-ray temperature; gravit. lenses

Mass in galaxies

Flat rotation curves (< 20 kpc): $M/L = (10 - 15)h$

$$GM/r^2 = v^2/r \quad \rightarrow \quad M(< r) \propto r$$

Satellite galaxy motion (to 200 kpc): $M/L \approx 200h$

gravit. lensing (to 260 kpc): $M/L \approx (150 - 250)h$

detection by LCRS and SDSS

The Milky Way

satellite galaxy motion (to 100 kpc): $M/L = 70$

Magellanic stream kinematics (50 kpc): $M/L \approx 50$

MW + M31 kinematics/timing: $M/L \approx 200$

Theoretical Argument: Disc stability

Disc is unstable: Need surrounding mass

SDSS – Mckay et al.

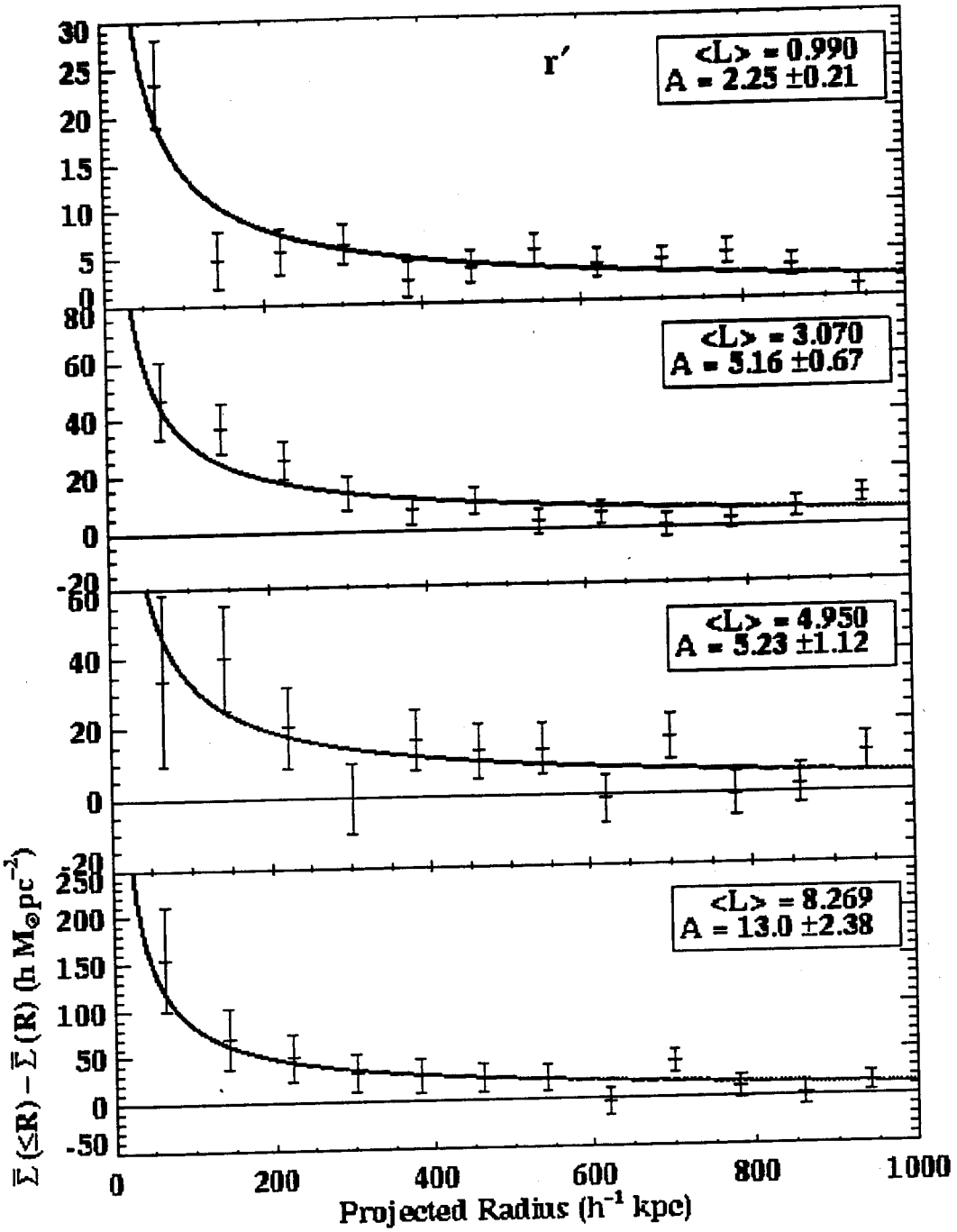

13.— GMCF in bins of r^* luminosity. Lines are the best fits to $R^{-0.8}$ power law models corresponding to the noted values of ılization A. Note that each plot has a different y-axis scale.

Baryon abundance vs. Total mass density

$\Omega_0 = 0.3 \pm 0.1$, as we discuss below

$\Omega_b = 0.04 \pm 0.015$ consistently from

nucleosynthesis

CMB

local baryon budget

CMB

The magnitude $\langle |\Delta T/T| \rangle \approx 10^{-5}$ is consistent with the structure formation only with $\Omega_0 \gg \Omega_b$

Consistent theory of structure formation fixes Ω_b/Ω_0

— Dark Matter cannot be baryon, nor massive neutrinos

$m_\nu > 30$ eV needed for haloes (cf. $m_\nu < 2.5$ eV)

No small-scale fluctuations

— Need it to be *Cold*

— Compact objects?

$(10^{-7} - 30) M_\odot$ objects are excluded by microlensing searches towards L/SMC

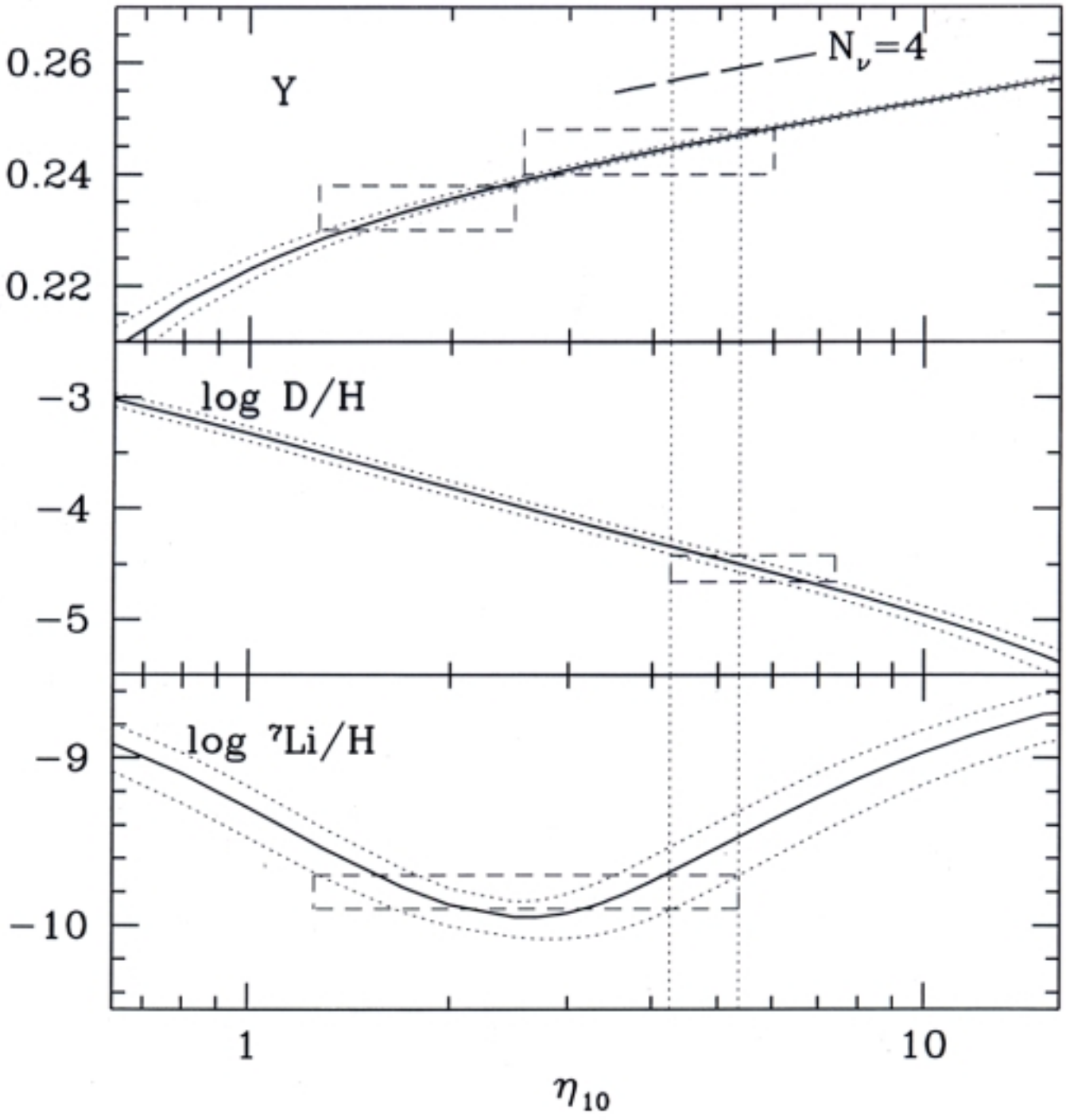
0.26
0.24
0.22
Y
N_ν=4
−3
−4
−5
log D/H
−9
−10
log ^{7}Li/H
1
10
η_{10}

CMB harmonics

$$C(\theta) = \sum_{\ell} C_\ell P_\ell(\cos\theta)$$

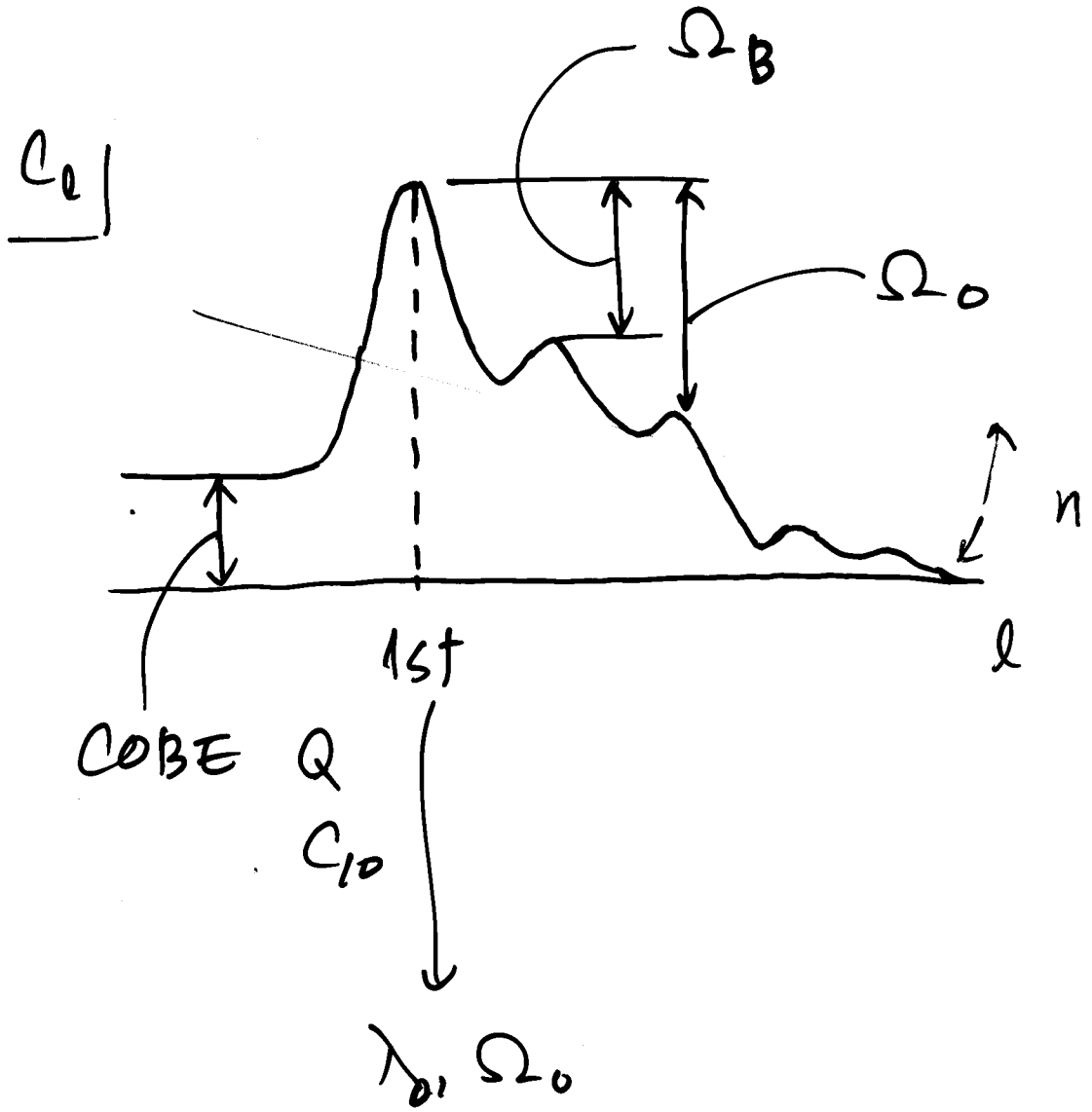

Hu, MF, Zaldarriaga, Tegmark ApJ 549, 669 (2001)

model : Hu, Fukugita, Zaldarriaga, Tegmark

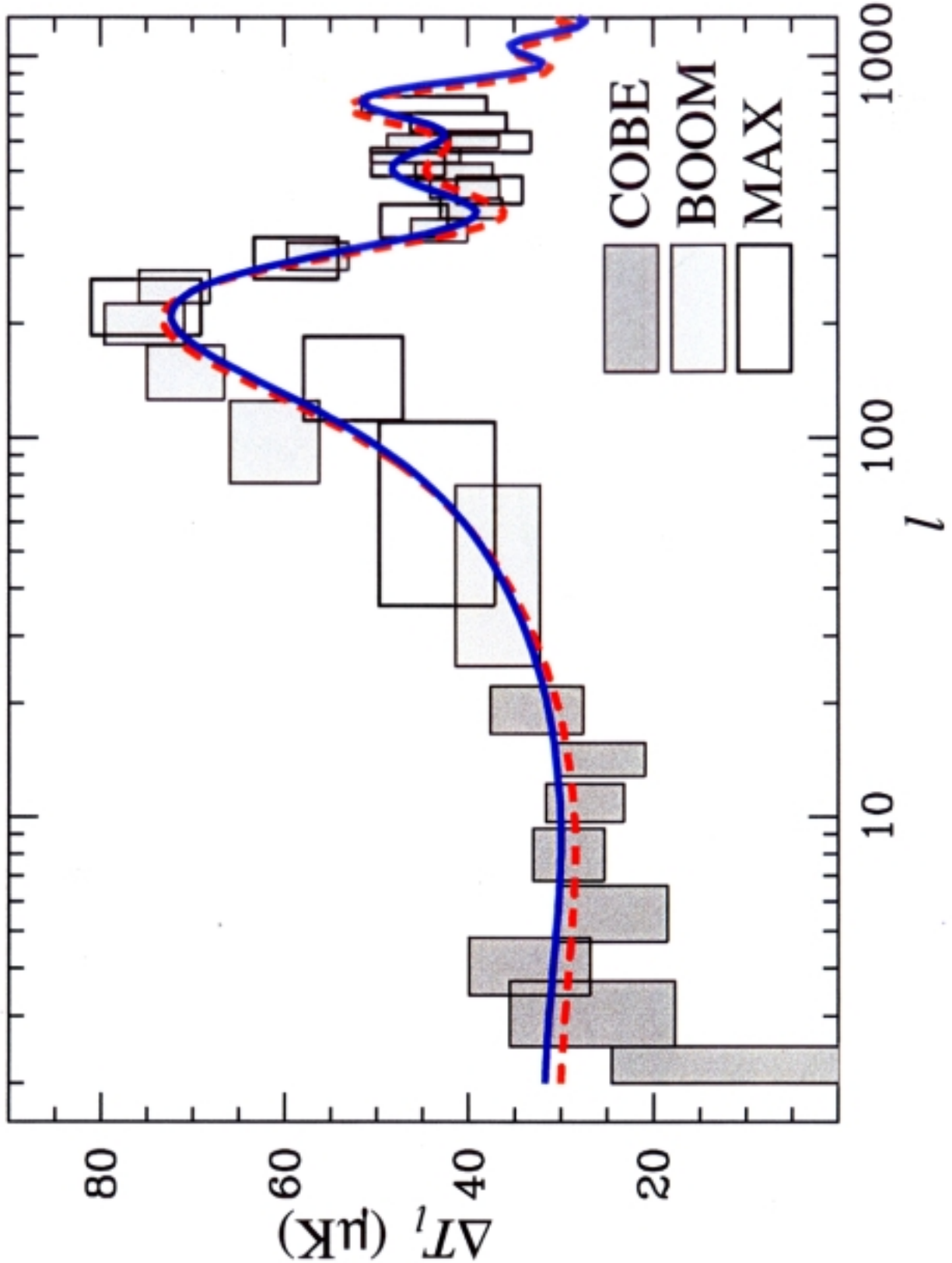

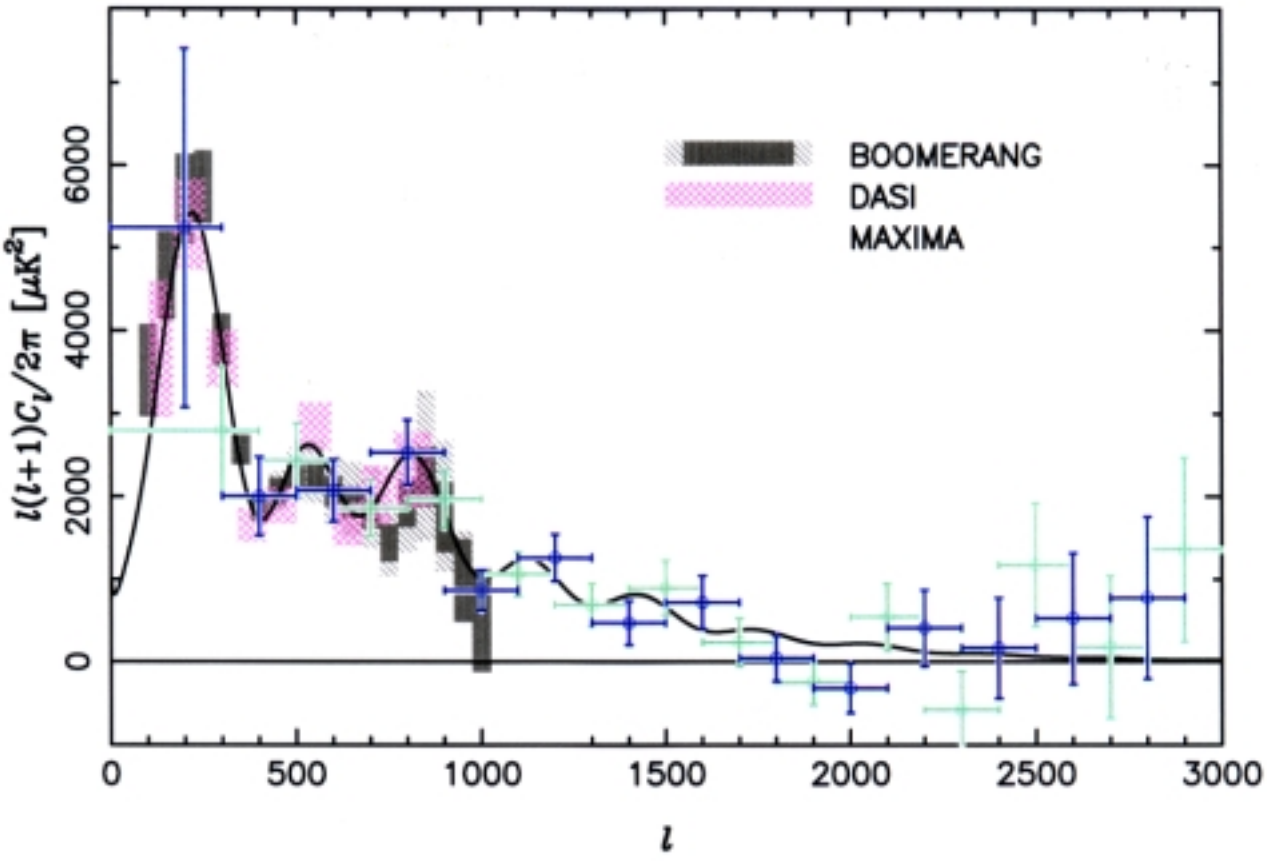

Fig. 1.— Features in the anisotropy spectrum (from Paper III). The first acoustic peak is seen at high sensitivity in the BOOMERANG (Netterfield et al. 2002), DASI (Halverson et al. 2002), and MAXIMA (Lee et al. 2001) observations, while the second and third acoustic peaks are seen at lower sensitivity (the rectangles indicate the 68% confidence intervals on band-power). The circles (dark blue) and squares (green) show the odd and even binnings of the CBI results from the joint spectrum of the three mosaic fields (see Paper III). The damping tail is clearly seen in the CBI spectrum, and, in the region of overlap, all four experiments are in excellent agreement, as is discussed in § 5.2. The black curve is the joint model also discussed in § 5.2.

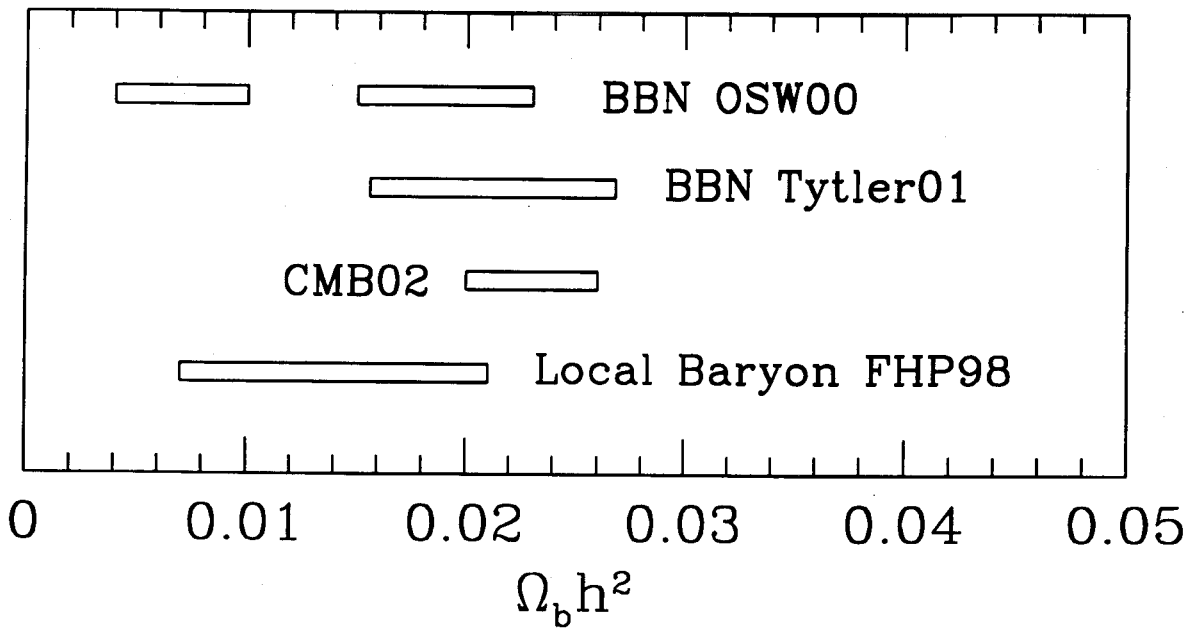
BBN OSW00
BBN Tytler01
CMB02
Local Baryon FHP98
0
0.01
0.02
0.03
0.04
0.05
$\Omega_b h^2$

Estimates of Ω_0

1. Luminosity density $\mathcal{L} \times \langle M/L \rangle$

   $\mathcal{L} = \int \phi(L) dL$, $\quad \phi(L)$: Luminosity function

   $\Omega_0 = 0.22 - 0.35$ from cluster

   $\Omega_0 = (0.13 - 0.22) \times 1.4$ from galaxy
   factor 1.4 for unclustered components

2. H_0 versus age

   $\Omega_0 < 1$

3. Type Ia supernova Hubble diagram

   $$\Omega_0 \approx 0.8\lambda_0 - 0.4$$

   $\Omega_0 = 0.1 - 0.5$ if flat

   $\Omega < 0.1$ if open

   — See below for possible systematic errors

4. Cluster baryon abundance

   $M_{\rm gas}/M_{\rm grav} = 0.056h^{-2/3}$ from X rays

   $[M_{\rm gas} + M_{\rm stars}]/M_{\rm grav} = \Omega_b/\Omega_0$

   means $0.3 < \Omega_0 < 0.5$

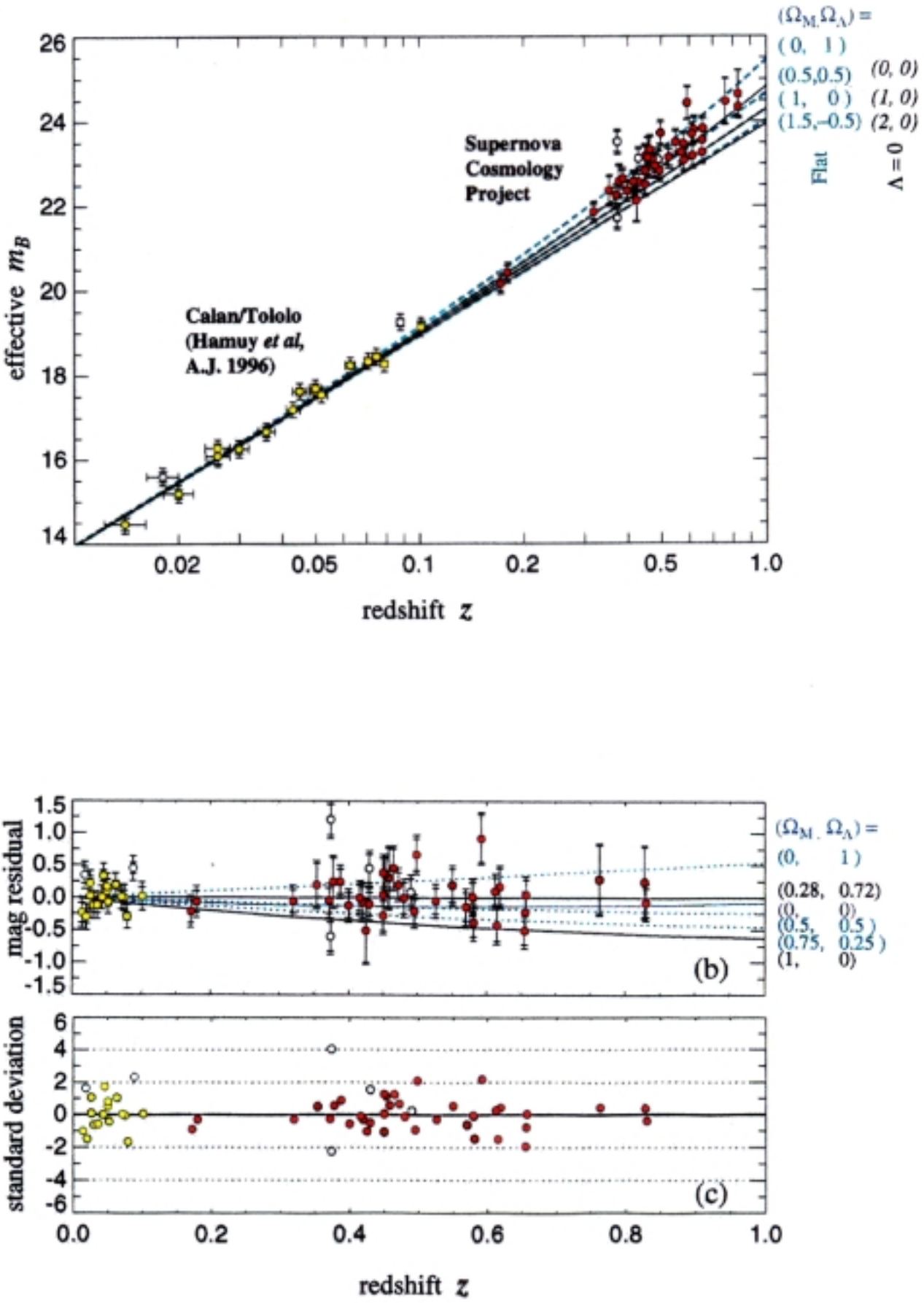
(ΩM, ΩΛ) =
(0, 1)
(0.5,0.5) (0, 0)
(1, 0) (1, 0)
(1.5,–0.5) (2, 0)
Flat
Λ = 0
Supernova
Cosmology
Project
Calan/Tololo
(Hamuy et al,
A.J. 1996)
effective m_B
redshift z
mag residual
standard deviation
(b)
(c)
(ΩM, ΩΛ) =
(0, 1)
(0.28, 0.72)
(0, 0)
(0.5, 0.5)
(0.75, 0.25)
(1, 0)

SN Cosmology Project

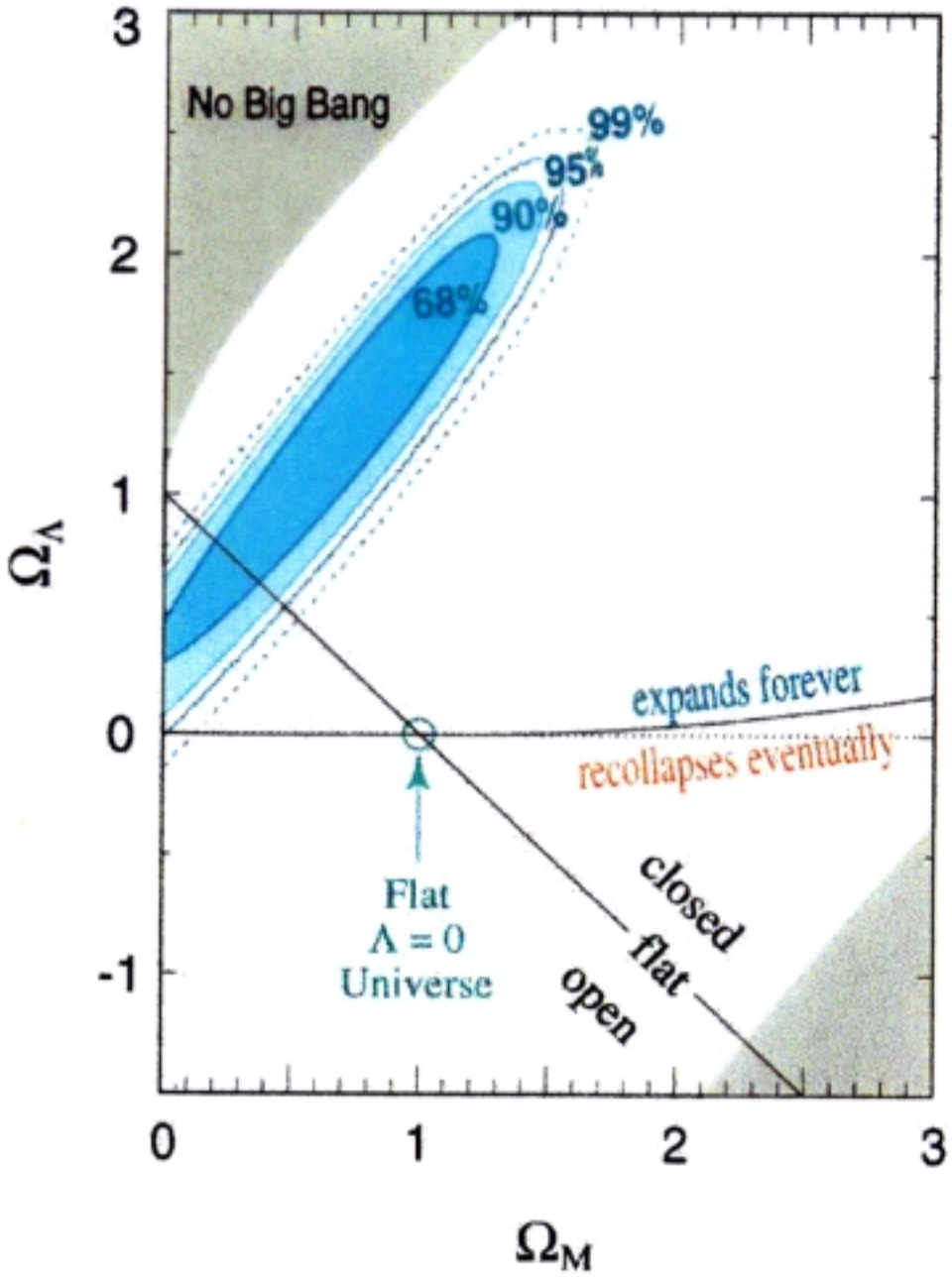

5. Peculiar velocity - density relation

$$\nabla \cdot \vec{v} + H_0 \Omega^{0.6} \delta = 0$$

small scale 10 kpc $\leq r \leq$ 1 Mpc

$\Omega_0 \approx 0.15 \pm 0.10$

large scale

$\Omega = 0.1 - 1$: the result controversial

6. Gravitational lensing frequencies
for splits of quasar images (strong lensing)

open universe: no constraints

flat universe: $\Omega > 0.2$

Structure-Formation-Model (w/ CDM) Dependent Determinations of Ω_0

7. Shape parameter of the Transfer Function

   $P(k) = k^n T(k, \Gamma)$

   $\Gamma \simeq \Omega h + (n_s - 1)/2 \qquad n_s = 1.0 \pm 0.05$

   $0.12 < \Gamma < 0.30 \quad \rightarrow \quad \Omega_0 = 0.15 - 0.45$

8. Rich cluster abundance at $z \approx 0$

   $\sigma_8 \approx 0.5\Omega^{-0.5}$

   8a. Matching with the CMB-COBE normalisation requires $\sigma_8 \approx 1$ and $\Omega \approx 0.25$

   8b. cluster mass function $\Phi(M)$ fits

   $\Omega_0 = 0.18 \pm 0.08$ and $\sigma_8 = 1 \pm 0.3$

   8c. Evolution of the rich cluster abundance

   $z \approx 0$ versus $z \approx 0.4 - 0.8$ (controversial)

   $\Omega_0 \approx 0.2 - 0.4$ (US, British)

   $0.5 \leq \Omega_0 \leq 1$ (French)

9. Cosmic shear of gravitational lensing

   $\sigma_8 \approx 0.5\Omega^{-0.5}$

   — the rest follows the same as (8)

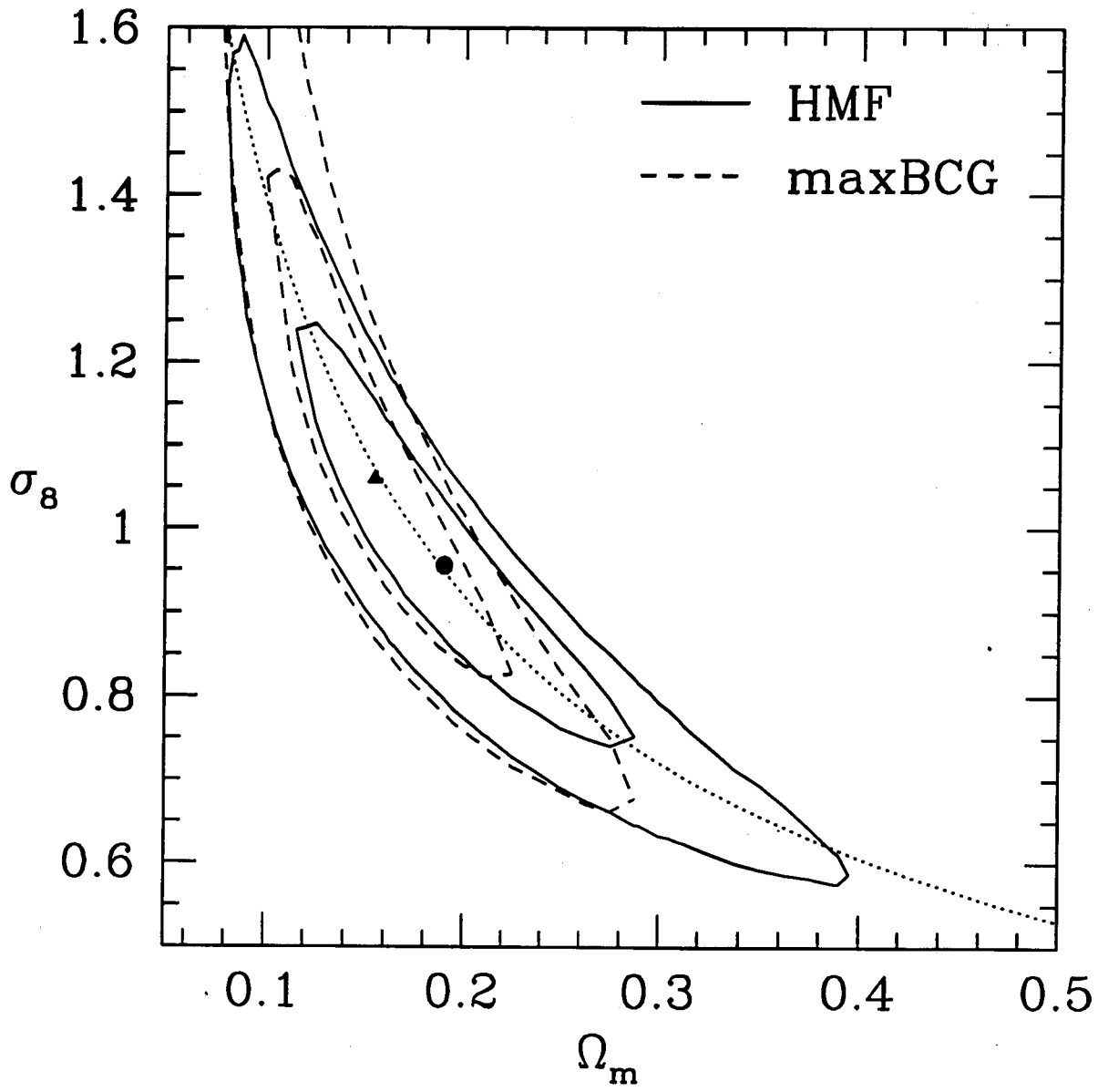

Fig. 5.— Allowed Ω_m- σ_8 range: one– and two– σ confidence contours for HMF (solid lines) and maxBCG clusters (dashed lines). The dotted curve is the best-fit relation $\sigma_8 = 0.35\Omega_m^{-0.6} \simeq (\frac{0.18}{\Omega_m})^{0.6}$. The best-fit Ω_m, σ_8 values are shown by the dark circle (HMF) and triangle (maxBCG).

10. Direct result from the CMB harmonics analysis

$\Omega = 0.44 \pm 0.20$ in a flat universe

$\Omega_0 = 0.3 \pm 0.1$ *is consistent with all determainations in a flat universe*

$\Omega \approx 1$ *contradicts with most observations*

NON-ZERO COSMOLOGICAL CONSTANT?

1. SNeIa Hubble Diagram

   Maximum brigheness of Type Ia Supernova is fainter than is expected in $\Lambda = 0$ universes

   $$f_{\max} = L_{\max}/4\pi d_L^2(z, \Omega_0, \lambda_0)$$

   Result: $\lambda_0 \approx 1.2\ \Omega_0 + 0.5$

   Caveat: problems of systematic errors (?)

   K-correction; colour band zero point matching; extinction in host galaxies

2. CMB: Position of the First Peak

$$\langle \frac{\Delta T(\theta)}{T} \frac{\Delta T(0)}{T} \rangle = \sum C_\ell P(\cos\theta)$$

$$\ell_1(\text{1st accoustic peak}) = \pi \frac{\text{distance to LSS}}{\text{sound horizon}}$$

Numerical calculation shows:

$$\ell_1 \approx 220 \sqrt{\frac{1-\lambda_0}{\Omega_0}}$$

Observations tell us $\ell_1 \approx 220$, so that $\Omega_0 + \lambda_0 \approx 1$

1997 vs 1999 data comparison (SN Cosmology Project)

SNe	1997	1999	1997−1999	2001
SN1992bi	(23.26±0.24)	23.11±0.46	(0.15)	.
SN1994H	22.08±0.11	21.72±0.22	0.36	.
SN1994al	22.79±0.27	22.55±0.25	0.24	.
SN1994F	(21.80±0.69)	22.26±0.33	(−0.58)	.
SN1994am	22.02±0.14	22.26±0.20	−0.24	.
SN1994G	22.36±0.35	22.13±0.49	0.23	.
SN1994an	22.01±0.33	22.58±0.37	−0.57	

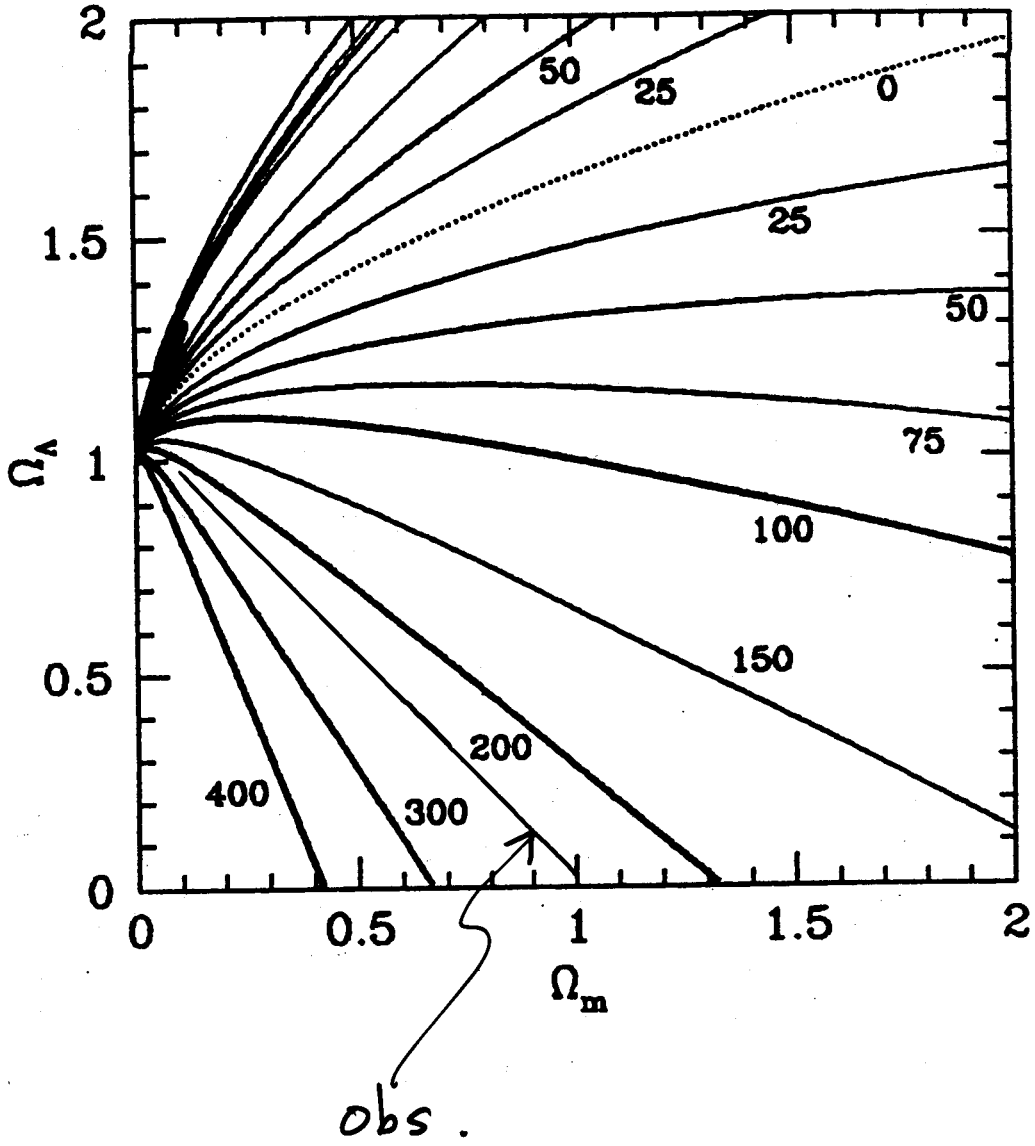
2
1.5
1
0.5
0
Ω_Λ
0
0.5
1
1.5
2
Ω_m
50
25
0
25
50
75
100
150
200
300
400
obs.

3. Strong Gravitational Lensing of Quasars

$$d\tau = F(1+z_L)^3\left(\frac{D_{LS}D_{OL}}{D_{OS}}\right)^2\frac{1}{(1+z_L)E(z_L)}dz_L$$

is very sensitive to Λ

So far $\lambda_0 > 0.8$ is excluded
considering system. errors from $F \sim n_G\sigma^4$

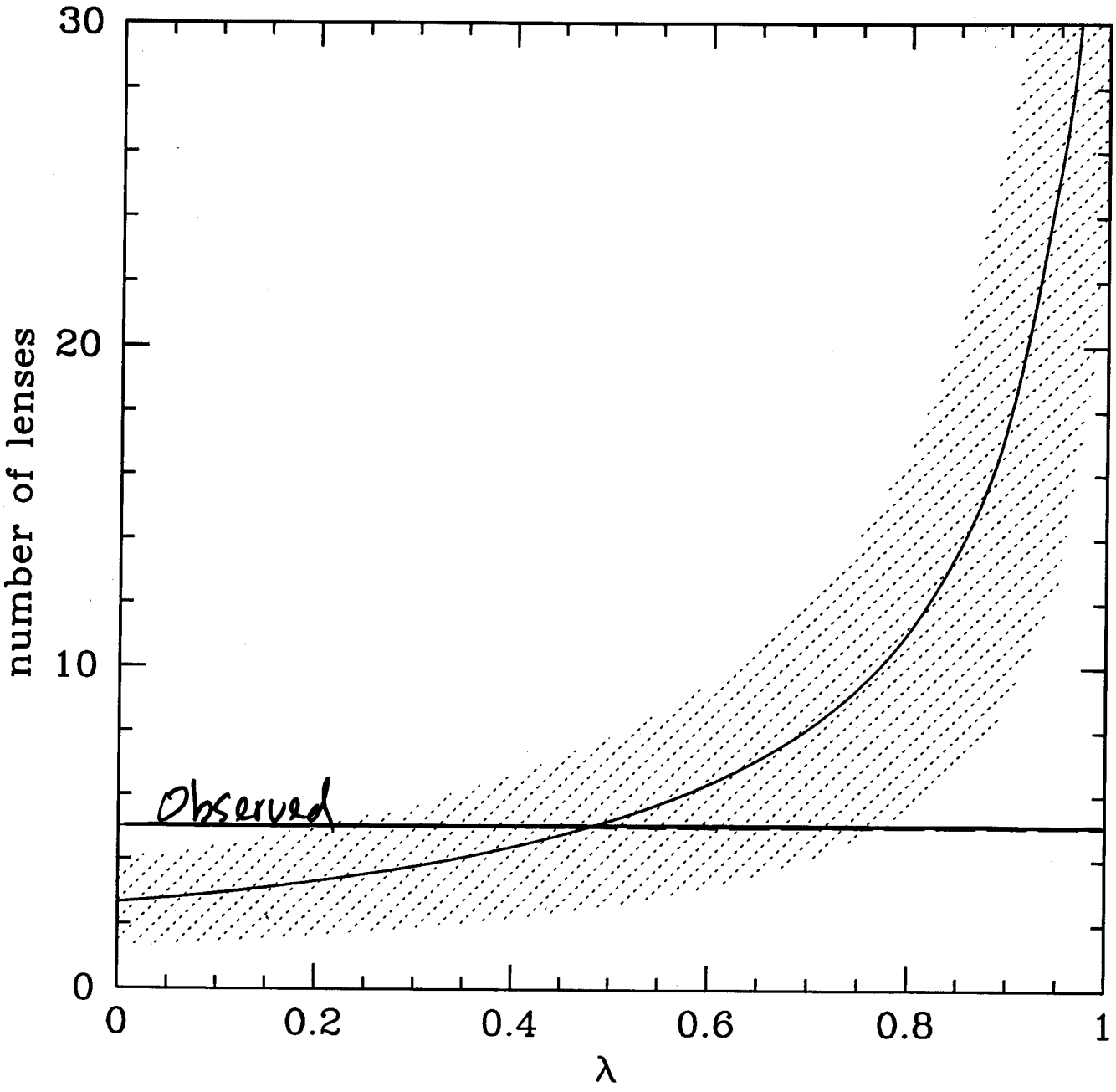
30
20
10
0
number of lenses
Observed
0
0.2
0.4
0.6
0.8
1
λ

CONCLUSIONS

1. Dramatic advancement for H_0
   especially by HST-KP for Cepheids, and
   better understanding of the nature of SNeIa

   HST-KP got $H_0 = 72 \pm 8$ km s^{-1}Mpc^{-1}.
   but the systematic error may be underestimated

   Most important error source: distance to LMC

2. Universe has low mass density (subcritical)
   - Model-independent determainations
   - CDM model-dependent determinations

3. Most of mass density comes from *Dark Matter*
   which is non-baryonic, non-neutrino, but *Cold*

4. Cosmological constant is non-zero (**CMB**, SNeIa)

   $$\Omega_0 + \lambda_0 \approx 1$$

5. The **concordance** parameters:

   $\Omega_0 \approx 0.3$; $\lambda_0 \approx 0.7$: $H_0 \approx 70$ km s^{-1}Mpc^{-1}

Flat: $\lambda_0 = 1 - \Omega_0$